Journal of The Electrochemical Society

The Electrochemical Society
Advancing solid state & electrochemical science & technology

OPEN ACCESS

Evaluation of Commercial Lithium-Ion Cells Based on Composite Positive Electrode for Plug-In Hybrid Electric Vehicle (PHEV) Applications: IV. Over-Discharge Phenomena

To cite this article: Matthieu Dubarry *et al* 2015 *J. Electrochem. Soc.* **162** A1787

View the article online for updates and enhancements.

You may also like

- Long–Term Aging – Overdischarge Degradation Mechanisms Interplay in Li-Ion Pouch Cells
Daniel Juarez-Robles, Judith A. Jeevarajan and Partha P. Mukherjee
- Copper Dissolution in Overdischarged Lithium-ion Cells: X-ray Photoelectron Spectroscopy and X-ray Absorption Fine Structure Analysis
Christopher E. Hendricks, Azzam N. Mansour, Daphne A. Fuentevilla et al.
- Overdischarge and Aging Analytics of Li-Ion Cells
Daniel Juarez-Robles, Anjul Arun Vyas, Conner Fear et al.

Your Lab in a Box!
The PAT-Tester-i-16: All you need for Battery Material Testing.
All-in-One Solution with integrated Temperature Chamber!
Cableless Connection for Battery Test Cells!
Fully featured Multichannel Potentiostat / Galvanostat / EIS!
www.el-cell.com +49 40 79012-734 sales@el-cell.com
EL-CELL®
electrochemical test equipment

This content was downloaded from IP address 3.133.144.217 on 25/04/2024 at 09:18

Evaluation of Commercial Lithium-Ion Cells Based on Composite Positive Electrode for Plug-In Hybrid Electric Vehicle (PHEV) Applications

IV. Over-Discharge Phenomena

Matthieu Dubarry,[a,*] Cyril Truchot,[a,c] Arnaud Devie,[a] Bor Yann Liaw,[a,*,z] Kevin Gering,[b] Sergiy Sazhin,[b,*] David Jamison,[b] and Christopher Michelbacher[b]

[a]*Hawaii Natural Energy Institute, SOEST, University of Hawaii at Manoa, Honolulu, Hawaii 96822, USA*
[b]*Idaho National Laboratory, Idaho Falls, Idaho 83415-2209, USA*

Lithium-ion cells with composite positive electrodes are attractive and promising for EV and PHEV applications. For powertrain applications, the battery packs are required to have multiple-cell configurations, where some battery management is needed to protect cells from experiencing overcharging and overdischarging. Here, we show how to analyze the effect of slight overdischarge in a graphite || $\{Li_xMn_{1/3}Ni_{1/3}Co_{1/3}O_2 + Li_xMn_2O_4\}$ cell, when it was overdischarged to 2.0 V. We found a peculiar behavior at low voltages that is imputable to the composite nature of the positive electrode. Under certain circumstances, due to differences in kinetic limitations in each of the constituents in the composite electrode, although $Li_xMn_{1/3}Ni_{1/3}Co_{1/3}O_2$ were discharged normally, $Li_xMn_2O_4$ could be overdischarged to $Li_2Mn_2O_4$ and cause capacity fade.
© The Author(s) 2015. Published by ECS. This is an open access article distributed under the terms of the Creative Commons Attribution Non-Commercial No Derivatives 4.0 License (CC BY-NC-ND, http://creativecommons.org/licenses/by-nc-nd/4.0/), which permits non-commercial reuse, distribution, and reproduction in any medium, provided the original work is not changed in any way and is properly cited. For permission for commercial reuse, please email: oa@electrochem.org. [DOI: 10.1149/2.0481509jes]
All rights reserved.

Manuscript submitted April 21, 2015; revised manuscript received May 18, 2015. Published June 20, 2015. This was Paper 1495 presented at the Boston, Massachusetts, Meeting of the Society, October 9–14, 2011.

Li-ion batteries with graphite intercalation compounds (G) as negative electrodes (NE) and mechanically blended compositions nominally denoted as $\{Li_xMn_aNi_bCo_cO_2$ (NMC) + $Li_xMn_2O_4$ (LMO)$\}$ as composite positive electrodes (c-PE) could be attractive for plug-in hybrid electric vehicle (PHEV) applications due to their ability of combining high power (rate capability) and high energy aspects.[1] To acquire sufficient understanding of the performance of this type of cells, studies on various subjects, including aging process and degradation mechanism, quantification of cell-to-cell variations (cell variability) among a small quantity of cells;[2] the rate capability over a range of rates;[2] quantification of attributes from various degradation modes to capacity fading in a 2C cycle aging regime;[3] and, the amount of reversible and irreversible capacity fading at different temperatures in a temperature excursion;[4] have been reported in our previous studies. Here, a study with illustrations of computer model-generated schematics on a peculiar overdischarge phenomenon was conducted to understand cell behavior against overdischarge protection. It is useful to characterize such overdischarge events to understand the impacts of such variations on battery control and management during the operation of battery packs. The understanding shall shed some light on the particular events and their effects with regard to the consequences on reliability and safety of the battery system. Eventually, it would be desirable that various degrees of overdischarge be characterized, as similar overdischarge events may occur in cells in a string or battery pack where intrinsic cell variability, extrinsically induced imbalance, and variations in the operating conditions such as under temperature gradients may present in a system. Although this particular overdischarge phenomenon may only be relevant to this c-PE cell design and chemistry, this mechanistic study shall address the general concern of possible overdischarging events in composite electrode design and performance and their consequence in capacity fade with composite electrode designs.

To receive a comprehensive understanding of this overdischarging behavior in the c-PE, one should refer to early studies of this family of materials, particularly the knowledge of the LMO compositions and their charge-discharge behavior in electrochemical cells. A useful reference is the review provided by Thackeray,[5] which summarized the various compositions in the Li-Mn-O ternary system and their behavior as active cathode materials in battery applications. The work reported by Jeong et al.[6] and by Wu and Yu[7] showed more current trends in utilizing such compositions in possible Li-ion battery applications. Although the exact composition in the commercial cells tested in this work was not known, the similarity in the cell behavior as revealed in the work of Jeong et al.[6] compared to ours gives us some basis for discussion to aid the understanding of the overdischarge behavior of the cell under evaluation in this work.

Experimental

A batch of thirty 1.9 Ah G || {NMC+LMO} (c-PE) commercial 18650 cells were used in this study. The cells were surveyed by an initial conditioning and characterization test using a Maccor 4300 battery tester to determine their performance characteristics and variations, as reported in Ref. 2. A nominal sample cell was subjected to a reference performance test (RPT) with discharge rates at C/25, C/5, C/2, 1C, 2C, 3C, 4C and 5C at 25°C in the voltage range of 4.25 V −2.0 V, which is different from the 4.2 V–2.8 V range specified by the manufacturer. There was a 4-h rest between any two subsequent steps in a test regime and the rest cell voltages (RCV) were recorded. The charge regime follows the recommendation by the manufacturer with a constant current step at C/2 to 4.2 V, followed by a constant voltage step until a cutoff current of C/25 was reached. To achieve better understanding of the overdischarge phenomenon, two additional cells were tested with charge-discharge cycles using C/25, C/5 and C/2 at −20°C in the following voltage ranges: 4.2–2.6 V and 4.2–2.3 V, respectively.

In addition, cells with each individual constituents of the c-PE (i.e. NMC and LMO, respectively) were evaluated using similar protocols. The results were used to understand if the overdischarge phenomena were originated from a specific constituent or stipulated by the nature of the composite electrode design. Commercial 1.95 Ah G || NMC and 1.2 Ah G || LMO cells from a different manufacturer were tested at 25°C with charge-discharge cycles at rates ranging from C/25 to 2C between 4.2 V and 2.0 V and with a 4-hour rest period at the end of each step in a test regime.

*Electrochemical Society Active Member.
[c]Present address: Aquion Energy, Pittsburgh, Pennsylvania 15201, USA.
[z]E-mail: bliaw@hawaii.edu

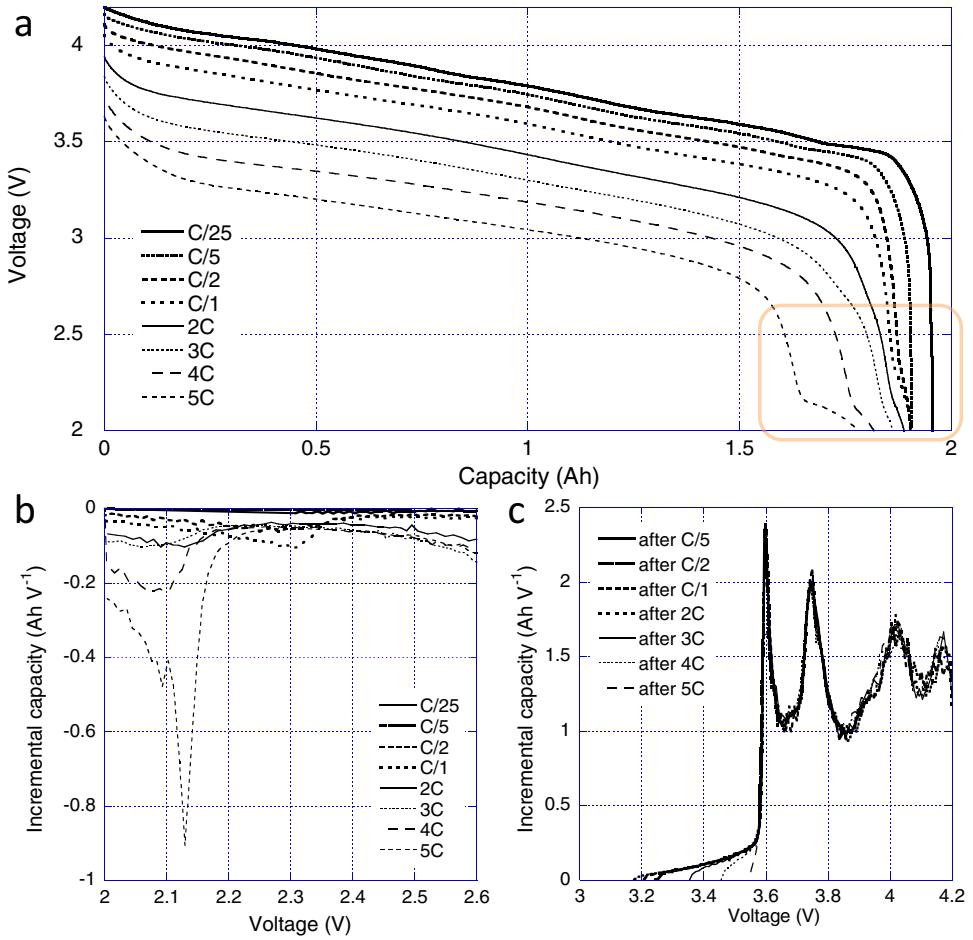

Figure 1. (a) Voltage vs. capacity discharges curves for the G || {NMC+LMO} cell from C/25 to 5C at 25°C, (b) the associated dQ/dV curves in the low voltage region, and (c) the dQ/dV curve of the subsequent C/2 charge regime.

Results

The overall performance of the c-PE cell at 25°C was comparable to those in the batch as reported previously.[1–3] Figure 1a shows that the most distinct feature on the discharge curves is in the highlighted region towards the end of discharge (EOD), where an excess capacity was exhibited with rates higher than C/5 and below 2.4 V at 25°C. The associated incremental capacity (dQ/dV) curves, as shown in Figure 1b, clearly show an additional reaction in the low voltage region below 2.4 V in the discharge regime. Interestingly, no clearly identifiable complementary dQ/dV peak appears in the subsequent C/2 charge regime as indicated in Figure 1c. Additionally, no anomaly was detected in the RCV measurements at the EOD or end-of-charge (EOC) in the tests either. This phenomenon is reproducible with other cells of the same batch in the same voltage range, which eliminates the possibility of involving incidents caused by cell variability, defects or artifacts from equipment or specific measurements. It is peculiar since the phenomenon only appears in the tests with rates higher than C/5; thus it is rate dependent and an indication of a kinetics-related issue. The dQ/dV peak position is also rate-dependent, corroborating the suspicion of kinetic origin. Furthermore, the capacity associated with this low-voltage reaction is higher with higher rates (e.g. from just 26 mAh at C/2 to 140 mAh at 5C).

Figure 2 presents the dQ/dV curves of two commercial cells, each comprising only a single constituent of the c-PE, i.e. (a) for NMC and (b) LMO PE. Each cell was tested in the 4.2 V–2.0 V range with rates ranging from C/25 to 2C. There was no excess capacity recorded in the low-voltage range in either case. It is therefore safe to assume that the excess capacity observed on Figure 1a in the low-voltage (<2.4 V) region must originate from the composite nature of the c-PE.

Figure 3a shows the incremental capacity (dQ/dV) versus cell voltage curves at C/25, C/5 and C/2 in the 4.2 V–2.3 V region at –20°C. In Figure 3a, some excess capacity is also observed in the low-voltage region below 2.5 V, however only in the C/25 and C/5 regimes. This excess capacity appears to be similar to the one observed at 25°C in the same voltage range but in the C/2 and 1C regimes. The cell performance characteristics as a function of temperature have been discussed in our previous work[4] and the differences in rate capability and polarization potential may have contributed to this observation that similar effects of excess capacity were measured at different voltages and with different magnitudes. The excess capacity is about 80 mAh at C/25 and 25 mAh at C/5 at −20°C. Similar to those observed at 25°C, no associated dQ/dV peak was observed in the charge regimes. Even at −20°C and C/25, the coulombic efficiency of the cycling is high, precluding the conjecture that this disparity between charge and discharge regimes on the excess capacity could attribute to a capacity loss due to side reactions, which should end up with a low coulombic efficiency. Were the excess capacity reversible, as shown by the high coulombic efficiency, the charge return associated with this excess capacity must have been incorporated into another dQ/dV peak, with a substantial voltage hysteresis that makes the peak position overlapped with that of another peak, indicating the disparity in kinetic pathways.

To address this possible voltage hysteresis, another cell was tested at C/25 under the same condition but in a narrower voltage range (i.e. 4.2 V–2.6 V). Figure 3b shows these two dQ/dV curves of different voltage ranges at C/25 for comparison. There are two distinctions between the two:

The dQ/dV peak associated with the last graphite intercalation staging reaction 2, 3, denoted as peak ❺ in Figure 3b, is more intense in the range of 4.2 V–2.3 V than in the 4.2 V–2.6 V range.

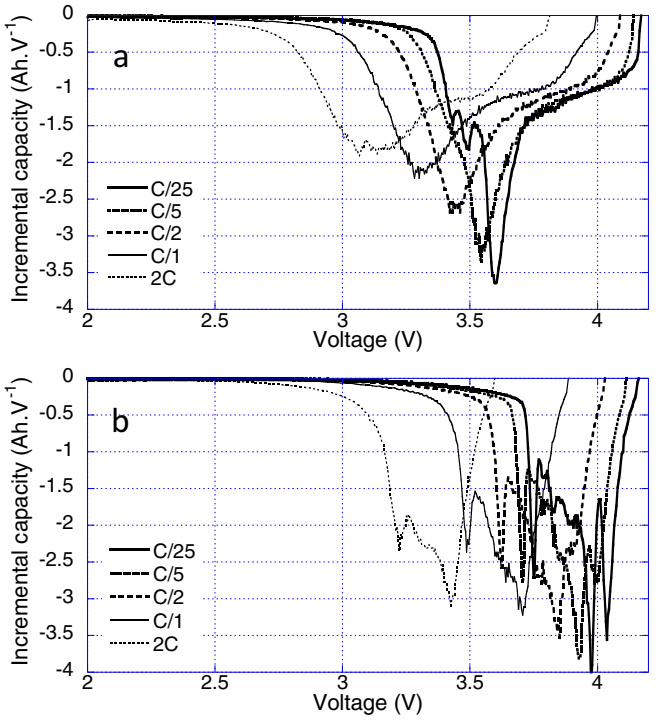

Figure 2. The dQ/dV curves in the discharge regimes from C/25 to 2C in the 4.2 V–2.0 V range for (a) a G || NMC cell and (b) a G || LMO cell at 25°C.

Additional peak intensity was recorded in the peak around 3.75 V, as noted by ∗ in Figure 3b.

Discussion

It seems that the presence of the additional electrochemical process is not a random event as it happened reproducibly under various circumstances. The absence of commensurate dQ/dV peaks in the low voltage range (<2.5 V) from either constituents of the c-PE versus a graphite electrode (Figure 2) suggests that this additional dQ/dV peak and its process are only related to the composite nature of the c-PE. The electrochemical behavior associated with this additional dQ/dV peak is peculiar, because it occurs at intermediate rates at room temperatures and at lower rates at lower temperatures, implying kinetic origins. Another peculiar aspect is that more capacity is released at higher rates. It was also observed that this excess capacity disappears after a few cycles at room temperature (not shown).

At this point, one should be mindful that the reaction pathway between the charge and discharge regimes might not be the same at −20°C and 25°C; thus, whether the results in Figure 1a and Figure 3a were associated with the same origin or not should be deciphered cautiously. The variations in the battery performance in the same range of discharge rates at −20°C and 25°C have been reported by us, as explained in Ref. 4. The reversible and irreversible variations in capacity and rate capability were discussed and no evidence of a different pathway was found with temperature disparity. The excess capacity at 25°C and −20°C occurred at about the same voltage below 2.5 V. The similarity in the behavior as portrayed by the shape of the discharge curves and the voltage range suggests that they are most likely related, although this phenomenon was observed at different rates (i.e. C/25 and C/5 at −20°C, while C/2 and 1C at 25°C). One should also be mindful that although the phenomenon was not observed for higher rates such as C/2 or 1C at −20°C, the shape of the discharge curves suggests that the polarization might be too high to show this phenomenon in the voltage range studied. In other words, if the cutoff voltages were extended to a wider voltage range to adjust for the polarization, the anomaly may become observable. Lastly, it

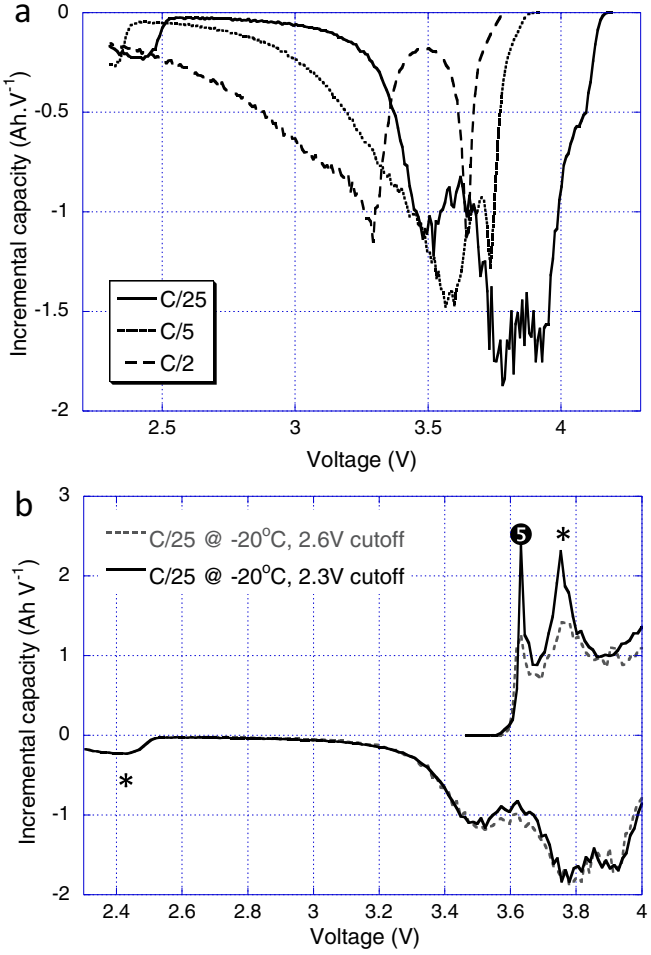

Figure 3. (a) The dQ/dV curve of a G || {NMC+LMO} cell tested at –20°C at C/25, C/5 and C/2 with a 2.3 V cutoff. (b) The dQ/dV curve of a C/25 cycle at –20°C for the same cell with a 2.3 V cutoff (solid line) and a 2.6 V cutoff (dotted line).

should be mentioned that a similar behavior was observed at C/25 at −5°C (not shown) and contributed 10 mAh to the cell capacity; but, not for temperatures above that.

Nature of the reaction.— How this excess capacity was created is puzzling and worth pondering. Were it a parasitic reaction at voltages <2.5 V, likely the excess capacity would be irreversible, which is not the case here. Another interesting observation is that at 25°C the excess reversible capacity increases with rate, which is counter-intuitive for any parasitic reaction. Furthermore, a parasitic reaction would be expected to slow down with reducing temperature, which was not observed here. All evidence suggests that this excess capacity does not come from an interfacial parasitic reaction. To yield a more comprehensible understanding of the nature of this process that gives excess capacity, we shall start with the results shown in Figure 3b and proceed with an incremental capacity analysis. Here, a more intensified peak ❺ in the charge regime suggests that the Li content in the NE has been depleted more previously at the EOD under this overdischarge process than a normal discharge regime; thus, the NE has released more Li for the excess capacity. Since the intensity of peak ❺ is a reflection of the degree of de-lithiation in the NE, this excess capacity could only be accomplished during discharge, resulting in an over-lithiation in the c-PE. Therefore, it implies that the reversible overdischarge process is associated with Li intercalation/deintercalation; thus, it is electrochemical. The additional area on the dQ/dV curve that represents the area of peaks (❺ + ∗) in the charge regime is commensurate with the

area of peak (∗) in the discharge regime, confirming the reversibility in terms of capacity with a large voltage hysteresis of more than 1 V at −20°C.

As the reaction was inferred to be electrochemical, the nature of such a reaction needs to be determined. In the literature, there is no specific discussion of a corresponding phase transformation in this voltage range for either NMC- or LMO-based cells with a graphite NE. This is affirmed by the results shown in Figure 2. As the PE is usually the capacity-limiting electrode, the initial lithium content in the PE shall be the maximum capacity of the cell. Therefore, no over-lithiation of PE should be expected in a normal discharging process. However, it is possible that certain transition metals could be reduced to a lower valence state at a lower potential against a Li/Li^+ reference electrode in the PE composition. For instance, it has been reported that $LiMn_2O_4$ (LMO) could be reduced to $Li_2Mn_2O_4$ slightly under 3 V vs. Li/Li^+ at equilibrium.[5,7] No lower-potential reductions were reported for NMC so far.

The voltage at which the excess capacity was observed in this work is lower than 3 V, where the LMO to $Li_2Mn_2O_4$ reaction may take place. However, since the cell uses a graphite NE, the voltage of the observed reaction should be further reduced and dependent on the state of de-lithiation of the NE. From Figure 3b, the reaction on NE associated with peak ❺ should occur near 0.22 V vs. Li/Li^+. Thus, the reduction of LMO to $Li_2Mn_2O_4$ should occur below 2.78 V at equilibrium in a cell with a graphite NE. This voltage should become even lower under polarization at higher rates and lower temperatures, consistent with the voltage range for the observed excess capacity in this work. From literature, the oxidation of $Li_2Mn_2O_4$ to LMO should occur in two steps: at 3.00 V and 3.50 V vs. Li/Li^+,[5,7] with a significant voltage hysteresis. This description corresponds well with the peak observed at 3.75 V (i.e. 3.50 + 0.22 V) in the charge regime in this study (as denoted by the peak ∗ in Figure 3b). The explanations support and corroborate the implications that in the c-PE, LMO was slightly over-lithiated under certain discharging conditions. Nevertheless, it remains puzzling if the LMO were over-lithiated, and the reaction capacity reversible, then an IC peak would be expected to appear near 2.8 V during charging. Why was such a peak not observed?

Kinetic origin.— As the over-lithiation of LMO being identified, it is interesting to know under what conditions it could happen. Although this LMO to $Li_2Mn_2O_4$ reaction has been reported in half-cell experiments for composite electrodes vs. a Li electrode,[6] where Li-ion is in excess; it is difficult to conceive how this over-lithiation of LMO could occur in a full cell, since the accessible Li content should be constrained by the initial Li content in the PE. In a typical discharge regime, at the EOD ideally all lithium ions should be retained in the PE where NMC and LMO are supposed to be fully lithiated to their respective state of charge, where kinetic charge balance or thermodynamic equilibrium could be attained.

As previously observed, the overdischarge process seems to be induced by certain kinetic limitations. It is worth investigating the kinetics of each constituents of the c-PE further. LMO is known to exhibit a higher rate capability than the mixed doped cobalt oxides[8] or NMC.[9] A plausible explanation, which might be overlooked in the past, is the degree of freedom introduced by the c-PE with regard to the reaction pathway. In the presence of the c-PE constituents and phases, the mechanical blending provides parallel reaction pathways (or current paths), through which each composition in the c-PE could react to different extents of Li content during the Li intercalation. In this case, since LMO is kinetically more favorable, it could end up with an "over-lithiated" state, while NMC suffers "under-lithiation." This scenario is a result of a delicate balance of thermodynamics and kinetics where the disparity in polarization between the two constituents may dictate the extent of the reaction commensurate with the potential under parallel pathways in the discharging regime, which leads to a disparity in compositions that do not follow those that were supposed to be dictated by the thermodynamic equilibrium. Furthermore, within the time frame of the test protocol, such equilibrium could not be attained in time by reversion of such a disparity from kinetic origin.

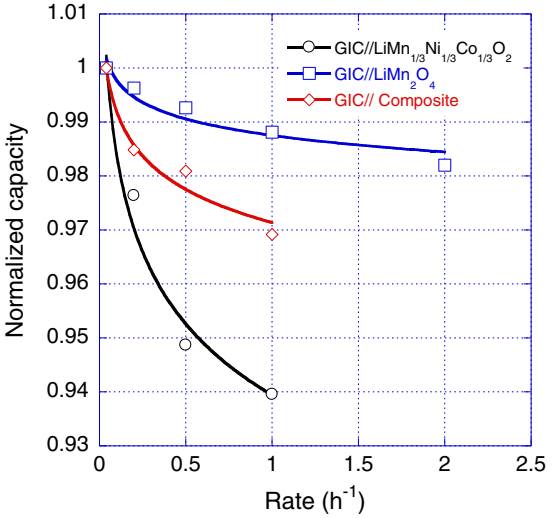

Figure 4. Peukert curves for three types of commercial cells: G || {NMC+LMO}, G || NMC, and G || LMO.

Such a "kinetic anomaly" could be investigated further in the observations in Figure 4 where the accessible capacity is compared as a function of discharge rate for three types of cells, that comprise (1) G || {NMC+LMO}, (2) G || NMC, and (3) G || LMO. In all three, the capacity variations follow the Peukert law with a Peukert coefficient significantly higher for the G || NMC cell at 1.02, compared to 1.004 for the G || LMO cell and 1.01 for the G || {NMC+LMO} cell. This observation suggests that NMC indeed could not handle higher rates as effective as LMO in these 18650-cell designs; but, this rate capability difference could be the results of either ohmic or faradaic (as related to the reaction kinetics) attributes, or both. It is possible to differentiate them by inferring the results shown in Figure 2a, where all IC intensities were close to zero at the EOD, implying that the capacity obtained at this cutoff condition is independent of the rate tested in the G || NMC cell. This observation also implies that the ohmic polarization attribute was not a deciding factor in capacity retention or coulombic efficiency. Thus, the rate capability and inefficiency in capacity release should be related to the NMC electrode kinetics. This remark is in agreement with the understanding in the literature that the kinetics of LMO is better than that of NMC. How such a kinetic disparity leads to the anomaly in the reaction pathways and results in the over-lithiation of LMO to $Li_2Mn_2O_4$ needs to be explained further.

Mechanistic understanding.— A useful exercise to visualize the conditions under which this over-lithiation of LMO could occur is to use a schematic illustration derived from simulations using *'alawa* model and toolbox[10,11] to provide a mechanistic explanation of how NMC and LMO work in the c-PE matrix during discharge. In Figure 5a, three schematic discharge curves at C/20, C/2, and 1C, are illustrated for NMC (top) and LMO (bottom), respectively, against a Li counter electrode in half-cell experiments. It should be noted that the capacity in the figures is normalized and scaled in proportion to the composition in the c-PE. As shown, the NMC exhibits a solid solution in the high-potential composition region and a phase transformation near 3.70–3.80 V where the intensity is more prominent at a lower rate. Since the NMC does not exhibit good rate capability, there is a significant capacity difference between the low and high rates. LMO has a better rate capability with three distinct potential plateaus, including the LMO-to-$Li_2Mn_2O_4$ one at about 2.80 V.

Figure 5b shows the schematic of a composite-electrode discharge curve with a {2/3 NMC + 1/3 LMO} composition[2] versus a Li reference electrode. As described in our previous work,[2] the Li intercalation in this composite electrode shall comprise a broad range of capacity

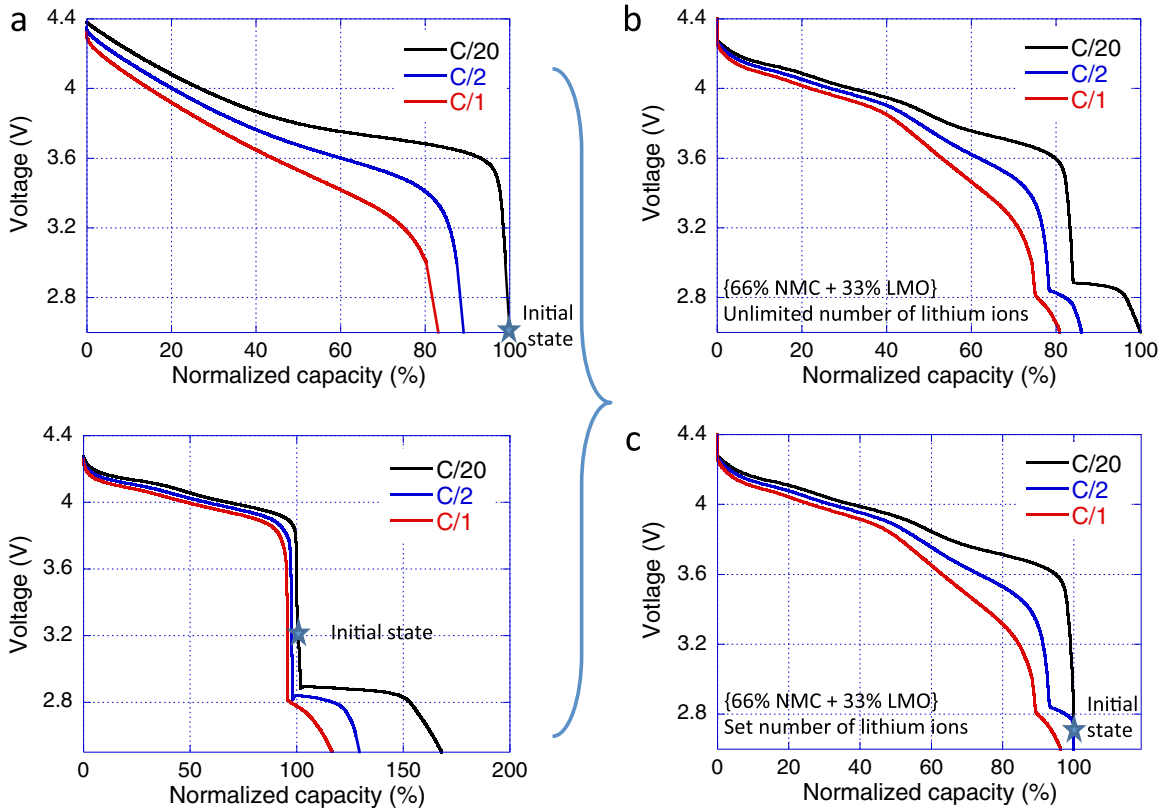

Figure 5. Schematic of the discharge curves synthesized from (a) the NMC and LMO discharge curves with half-cell potential vs. Li/Li$^+$ to (b) the resulting c-PE of a {2/3 NMC + 1/3 LMO} composition with unlimited source of Li-ions supply and (c) the c-PE of the same composition but with limited supply of Li-ions from the NE.

rendering the solid solution region of the NMC that also encompasses the first two LMO phase transformations prior to the NMC phase transformation. If the EOD cutoff voltage were extended below 3 V, the Li reaction with NMC shall also incorporate the third LMO phase transformation. In a Li-ion cell, as shown in Figure 5c, since the c-PE was assembled with LMO in the $LiMn_2O_4$ composition (★'s on Figure 5), the number of Li ions available for reaction in the cell is finite; thus, a discharge with over-lithiation at C/20 is not possible, since the capacity is constrained. However, as rate increases, given the difference in rate capability while constraining the amount of Li ions for reaction, the over-lithiation of LMO to $Li_2Mn_2O_4$ is possible for medium rates. The schematic shows that, because of the poor rate capability of NMC, remnant Li ions could become available to further reduce LMO to $Li_2Mn_2O_4$ prior to the cutoff. It also shows that, because of the over-lithiation of LMO to $Li_2Mn_2O_4$, the capacity of C/2 could be similar to that of C/20. One should be mindful that in the full cell the actual amount of Li ions that are accessible for the over-lithiation of LMO could also depend on the rate capability of the NE. The rate capability of the NE is usually so high that it should not affect the degree of over-lithiation of LMO; thus, this scenario was not considered in our simplified schematic representation.

The schematic shown in Figure 5c should also explain the dependence of excess capacity as a function of rate. As exemplified, under the constraint of limited amount of Li ions for discharge, the LMO over-lithiation could not be completely accomplished at 1C, but it is near completion at C/2. Thus, the full capacity could be released at C/2, but not at 1C. The schematic implies that, on one hand, the higher the rate, the fewer amounts of Li ions were accommodated in the NMC reaction; thus, the more ended up in the LMO over-lithiation. On the other hand, as the rate increases, the extent of the LMO over-lithiation could be also limited to deliver full capacity.

There is one remaining aspect of this peculiar overdischarge phenomenon that needs explanations: the disappearance of the overdischarge process after a few cycles. We shall begin with the cell degradation mechanisms. It is known that the main degradation mode of this cell chemistry is the loss of lithium inventory (LLI).[3] Under this degradation mode, graphite should be fully delithiated before the NMC becoming fully lithiated; thus, it leaves no excess Li ions for the LMO over-lithiation. This is the "slippage," as described in Ref. 11, as the mechanism of which the NE continues to move toward higher SOCs, while the capacity slips gradually. Figure 6a is a schematic to illustrate this slippage process and the consequence for the disappearance of the over-lithiation of LMO. In the beginning, as indicated by the arrow on the right for the 2.3 V cutoff at the EOD, which was triggered by the rise of the NE potential that led to the voltage cutoff, while the c-PE potential remained on the LMO over-lithiation plateau. As the LLI continued to incur, accompanying with the NE slippage, the LMO over-lithiation could disappear when a certain level of the LLI has occurred, as shown in Figure 6a by the left arrow for the cutoff at 2.3 V. This explanation on the disappearance of the LMO over-lithiation is irrelevant to the structural reversibility issues discussed in Ref. 5 regarding the Li site occupancy and its transition in the layered and spinel structures with LMO. The disappearance of LMO over-lithiation could be just a result of the normal aging of the cell. In contrast, an arrow showing a 2.8 V cutoff in the beginning of life is also illustrated in Figure 6a to exhibit why over-lithiation of LMO is not possible under a normal discharge regime.

As a final remark, it remains interesting to know why the over-lithiation did not occur in the G || LMO cell, even with a 2 V cutoff. As illustrated in the bottom figure of Figure 5a, it suggests that a <2.7 V cutoff is sufficient to observe the over-lithiation plateau. At a 2.8 V cutoff, a slight over-lithiation could occur at C/20, since a sufficient amount of Li might be available. In a full cell configuration, however, it is known that the graphite NE shall engage irreversible capacity loss in the first cycle, as an offset should be introduced in the estimation of SOC, as described in Ref. 11. This offset shall prevent any possible

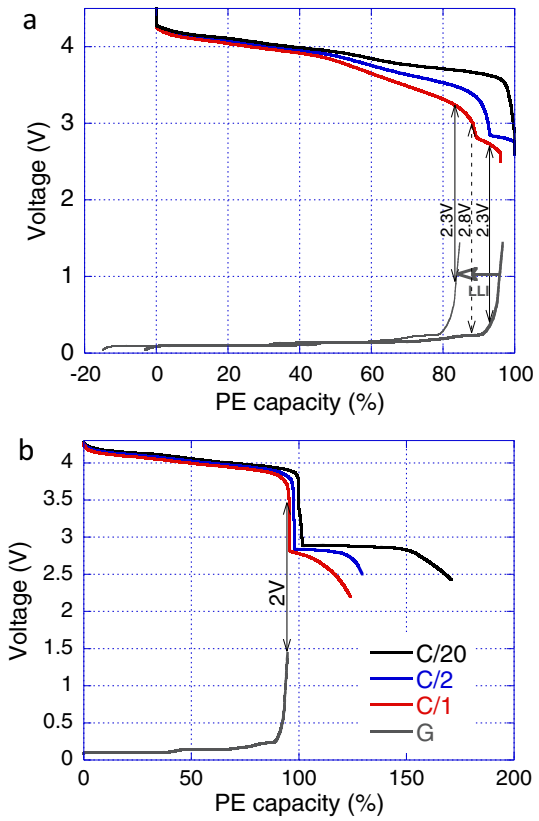

Figure 6. (a) A schematic showing the effect of loss of lithium inventory on the capacity fade when c-PE experienced overdischarge. (b) A schematic showing a G || LMO cell and why overdischarge is not possible in this configuration even at 2 V.

over-lithiation of LMO, as shown in Figure 6b. It is because the cutoff shall be reached prior to the over-lithiation of LMO. In other words, because the G || LMO cell is limited by the capacity constraint imposed by the NE at the EOD, the over-lithiation of LMO is not possible. In the case of a G || NMC cell, the capacity at the EOD is usually constrained by the PE above certain rates (due to the poor rate capability of NMC that often triggers the cutoff). This is what opens up the possibility of over-lithiation of LMO in a c-PE.

Conclusions

The peculiar overdischarge phenomenon and its effects on the performance of a composite $\{LiMn_{1/3}Ni_{1/3}Co_{1/3}O_2 + LiMn_2O_4\}$ Li-ion cell were investigated using incremental capacity analysis as an electrochemical inference method. A reversible over-lithiation of $LiMn_2O_4$ to $Li_2Mn_2O_4$ reaction was found to produce excess capacity as a function of rate under certain circumstances. Although this reaction is not supposed to occur under normal discharge condition, given the amount of Li ions was constrained by the composition of the composite positive electrode in the system, it was proved that it could occur due to the difference in rate capability between LMO and NMC. The poor rate capability of the NMC in the composite positive electrode avails some of the Li ions for over-lithiation of LMO. Because of its kinetic origin, this excess capacity was accessible only at rates above a threshold at a temperature. Moreover, this over-lithiation of LMO could disappear in cycle aging. This phenomenon could be accounted for by the main degradation mode, the loss of lithium inventory; and not necessarily related to the limited reversibility of the LMO to $Li_2Mn_2O_4$ reaction, as suggested in the literature.

Acknowledgments

The authors would like to gratefully acknowledge the funding provided by the Office of Energy Efficiency and Renewable Energy (EERE) of the U. S. Department of Energy (Contract No. DE-AC07-05ID14517).

References

1. K. L. Gering, S. V. Sazhin, D. K. Jamison, C. J. Michelbacher, B. Y. Liaw, M. Dubarry, and M. Cugnet, *J. Power Sources*, **196**, 3395 (2011).
2. M. Dubarry, C. Truchot, M. Cugnet, B. Y. Liaw, K. Gering, S. Sazhin, D. Jamison, and C. Michelbacher, *J. Power Sources*, **196**, 10328 (2011).
3. M. Dubarry, C. Truchot, B. Y. Liaw, K. Gering, S. Sazhin, D. Jamison, and C. Michelbacher, *J. Power Sources*, **196**, 10336 (2011).
4. M. Dubarry, C. Truchot, B. Y. Liaw, K. Gering, S. Sazhin, D. Jamison, and C. Michelbacher, *J. Electrochem. Soc.*, **160**, A191 (2013).
5. M. M. Thackeray, *Prog. Solid State Chem.*, **25**, 1 (1997).
6. S. K. Jeong, J. S. Shin, K. S. Nahm, T. P. Kumar, and A. M. Stephan, *Mater. Chem. Phys.*, **111**, 213 (2008).
7. S.-h. Wu and M.-t. Yu, *J. Power Sources*, **165**, 660 (2007).
8. P. Albertus, J. Christensen, and J. Newman, *J. Electrochem. Soc.*, **156**, A606 (2009).
9. N. Yabuuchi and T. Ohzuku, *J. Power Sources*, **119–121**, 171 (2003).
10. https://www.soest.hawaii.edu/HNEI/alawa/
11. M. Dubarry, C. Truchot, and B. Y. Liaw, *J. Power Sources*, **219**, 204 (2012).